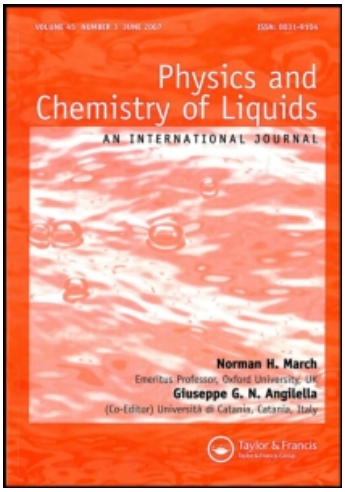

Physics and Chemistry of Liquids
Publication details, including instructions for authors and subscription information:
http://www.informaworld.com/smpp/title~content=t713646857

Different solidification behaviours of Bi-10wt%Te alloy induced by liquid structural change

Zhong-Yue Huang[a]; Fang-Qiu Zu[a]; Yan-Fa Han[a]; Zhong-Hua Chen[a]; Zhi-Zhi Wang[a]
[a] Liquid/Solid Metal Processing Institute, School of Materials Science and Engineering, Hefei University of Technology, Hefei 230009, P.R. China

Online publication date: 10 December 2010

To cite this Article Huang, Zhong-Yue , Zu, Fang-Qiu , Han, Yan-Fa , Chen, Zhong-Hua and Wang, Zhi-Zhi(2010) 'Different solidification behaviours of Bi-10wt%Te alloy induced by liquid structural change', Physics and Chemistry of Liquids, 48: 6, 699 — 707
To link to this Article: DOI: 10.1080/00319100902913197
URL: http://dx.doi.org/10.1080/00319100902913197

Physics and Chemistry of Liquids
Vol. 48, No. 6, December 2010, 699–707

Taylor & Francis
Taylor & Francis Group

Different solidification behaviours of Bi–10wt%Te alloy induced by liquid structural change

Zhong-Yue Huang, Fang-Qiu Zu*, Yan-Fa Han, Zhong-Hua Chen and Zhi-Zhi Wang

Liquid/Solid Metal Processing Institute, School of Materials Science and Engineering, Hefei University of Technology, Hefei 230009, P.R. China

(*Received 26 February 2009; final version received 21 March 2009*)

By means of DC four-probe technique, the temperature dependence of the electrical resistivity (ρ–T) of liquid Bi–10wt%Te alloy has been measured. Two abnormal changes on the ρ–T curve within the temperature ranges of 497–550°C and 639–708°C suggested that two irreversible liquid–liquid structural changes (LLSC) occurred. To explore the effects of the LLSC on the solidification behaviour of the alloy, solidification experiments were carried out. The results show that after experiencing LLSC, there will be enlarged undercooling, much finer microstructures and larger quality of Bi_2Te phase. Moreover, the morphology of solidified Bi_2Te is changed from dendrite to equiaxed.

Keywords: Bi–10wt%Te; liquid–liquid structural change; solidification; undercooling

1. Introduction

Although melt superheating treatment has been widely used in modifying the solidification microstructure and improving the physical properties of various materials [1–5], the underlying mechanism and functioning rules are still unclear for it is difficult to observe the liquid structure directly. As known, the structure of liquid has direct influences on the microstructure and properties of materials. Therefore, exploring the structure of the liquid to research the microstructure and property of material is possible and needed.

Based on results of the X-ray diffraction studies on liquid Sn–Zn, Sn–Pb and Bi–Pb eutectic systems performed by Danilov and Radchenko [6], the structure of molten alloys at the temperature not far above liquidus is considered as micro-heterogeneous. Later, similar results were obtained for other eutectic systems using X-ray, electron and neutron diffraction. Signs of an analogous microinhomogeneity were also observed during investigations of melts in systems with monotectics above their macroscopic stratification cupola. The existence of the microinhomogeneity was partly missing during heating process [7]. In a previous work for PbSn eutectic alloy by various methods such as revised internal friction technique [8], electron diffraction [9], neutron diffraction [9], differential thermal analysis (DTA) [10],

*Corresponding author. Email: fangqiuzu@hotmail.com

ISSN 0031–9104 print/ISSN 1029–0451 online

DOI: 10.1080/00319100902913197
http://www.informaworld.com

differential scanning calorimetry (DSC) [10], DC four-probe method [11] and viscosity measurement [12], a liquid–liquid structure change(LLSC) has been proven to occur at a temperature much above liquidus. The similar phenomena have also been observed in some alloy melts, e.g. Pb–Bi [13], Sn–Sb [14], In–Sn [15] and some others. Furthermore, the solidification microstructures of Pb–Sn [16], Bi–Sb [17] and Al–Si [18] were changed greatly as LLSC happened.

The semiconducting V2–VI3 compounds have been studied for more than three decades, because these compounds have properties that make them important for technological applications in thermoelectric power conversion as well in the fabrication of Hall effect devices [19]. In particular, bismuth telluride and its alloys are known as one of the best thermoelectric (TE) materials currently available near room temperature, their highest figure of merit $ZT \approx 1$ ($ZT = (*^2\sigma/\kappa)T$, where $*$, σ and κ are Seebeck coefficient, electric conductivity and thermal conductivity of the material, respectively, and T is the absolute temperature; most modern TE coolers, thermal sensors or other devices and so on, are made from such materials [20].

In this article, we chose Bi–10wt%Te to carry out experiments. Interestingly, we observed the phenomenon of two irreversible LLSC occurring in Bi–10wt%Te during heating process with the help of DC four-probe method. Moreover, the solidification behaviours and resulted microstructures of Bi–10wt%Te alloy are quite different when solidified from dissimilar liquid states (before and after LLSC).

2. Experimental procedures

2.1. *Electrical resistivity measurements*

For exploring the pattern of electrical resistivity versus temperature, i.e. ρ–T of the melt Bi–10wt%Te, DC four-probe method was used. Samples composed of pure Bi (99.9%) and Te (99.99%) were melted at 470°C for 30 min; during entire melting process, the samples covered with shielding flux were shaken mechanically three times for component homogenisation. Then they were poured into measuring cells manufactured from silica glass, 3.38 mm in diameter. The thermal expansion of the

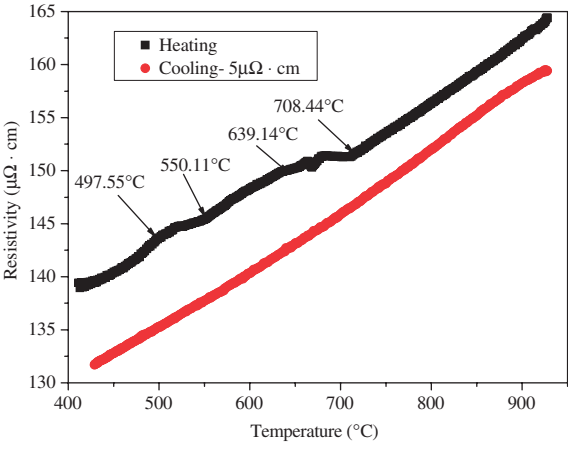

Figure 1. Electrical resistivity ρ as function of temperature for Bi–10wt%Te.

silica glass was so small that the size variation with temperature could be neglected. Four tungsten electrodes, 1 mm in diameter, two for current and two for voltage, were placed in the orifices of the cell up-wall. The voltage was measured by a KEITHLEY-2182 nanovoltmeter with constant current of 500 mA supplied by a PF66M sourcemeter. The experimental details and the set-up have been described elsewhere [11]. Experiments were carried out in highly purified argon for preventing the samples from oxidation. In each experiment, we studied the temperature dependence of electrical resistivity of the samples by heating and cooling both at a rate of $10^{\circ}C\,min^{-1}$. The error of the system is under 2%, and we obtained reproducible results in the repeated measurements. After electrical resistivity measurements, we checked tungsten electrodes, and no chemical reactions were found.

2.2. *Solidification experiments*

To explore function rules in solidification caused by different liquid structure states before and after it experienced LLSC, melting and holding temperatures for the alloys are chosen according to the temperature range with anomalous changes of physical properties mentioned above (Figure 1), and the temperature treatments of liquid alloys were conducted by the following sequential scheme (Figure 2): four samples A, B, C and D with identical compositions and weights were prepared. Sample A and B were held at 470°C and 570°C for 30 min, respectively, and then cooled in air. Sample C was held at 570°C for 30 min, then rapidly cooled to 470°C, held 30 min, cooled in air at last. Sample D was held at 750°C for 30 min, then rapidly cooled to 570°C, held 30 min, cooled in air finally. During the entire melting process, the samples covered with shielding flux were shaken mechanically three times for component homogenisation. At the same time, the cooling curves (T–t) were recorded by a KEITHLEY-2182 nanovoltmeter and computer collection system with a NiCr–NiSi thermocouple protected by quartz sheath located at the same distance of 10 mm from the bottom of the crucible. The error of the system is under 1%. After that, each sample was weighed before and after the LLSC, and we

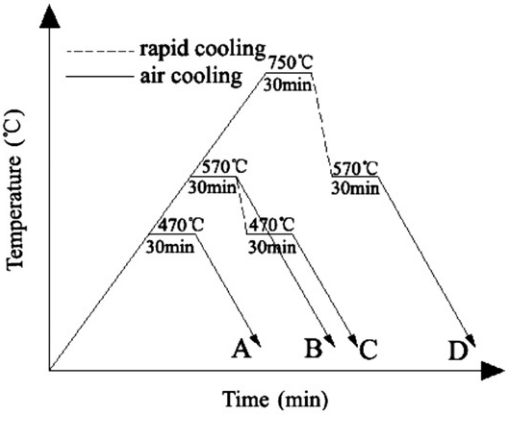

Figure 2. Sketch of preparation procedure of Bi–10wt%Te.

observed only a slight loss (of less than 0.01g) of mass. The solidified specimens were used for structure and phase examinations by the optical morphology method.

3. Experimental results

The patterns of resistivity versus temperature (ρ–T) of Bi–10wt%Te melt are shown in Figure 1. The electrical resistivity of liquid Bi–10wt%Te alloy changes abnormally within the temperature ranges of 497–550°C and 639–708°C during the heating process. Owing to the sensitivity of electrical resistivity to structure of material, such abnormal change of the electrical resistivity reflects existence of LLSC in the investigated melt. But in the cooling process, it changes linearly. This indicates that LLSC of Bi–10wt%Te is irreversible.

The cooling curves of the four samples are shown in Figure 3, and the related solidification parameters are shown in Table 1. It can be seen that the four samples have different characteristic temperatures. For example, the primary phase nucleate undercooling of sample D is about 6°C higher than that in others. The results

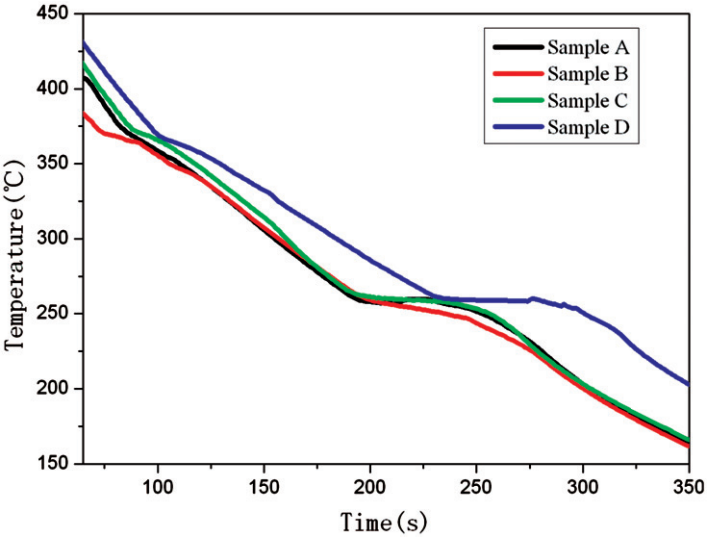

Figure 3. Cooling curves for Bi–Te melts.

Table 1. Characteristic temperature in cooling curve of Bi–10wt%Te.

Samples	T_S (°C)	ΔT_S (°C)	T_E (°C)	ΔT_E (°C)
A	372.96	3.04	260.27	5.73
B	371.79	4.21	259.67	6.33
C	372.40	3.60	261.35	4.65
D	366.81	9.18	260.92	5.08

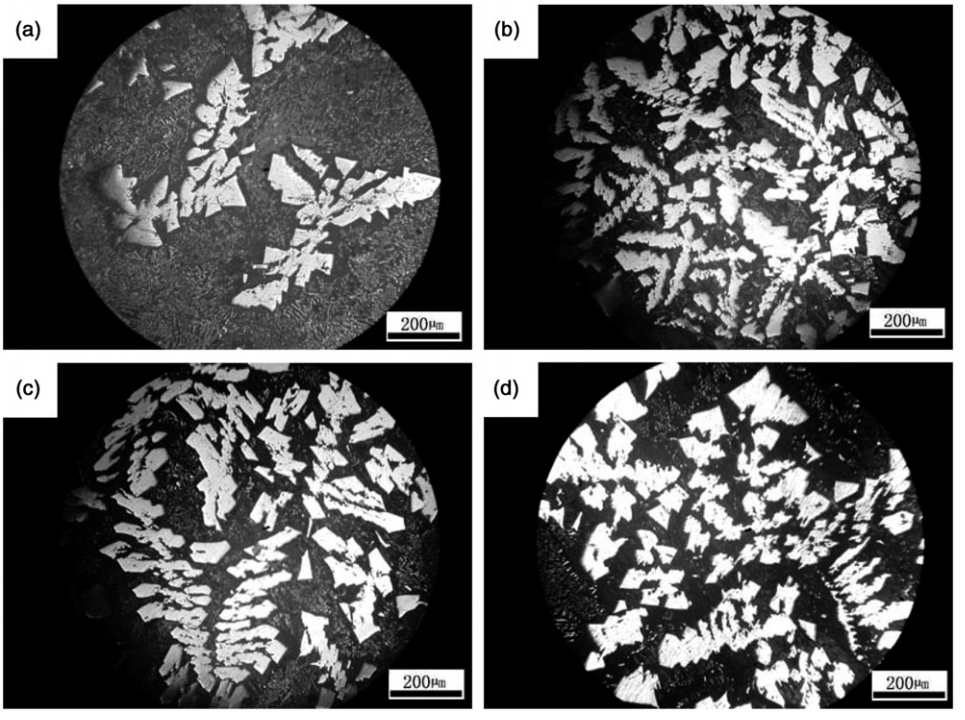

Figure 4. Solidification microstructures of Bi–10wt%Te: (a) melted at 470°C, (b) melted at 570°C, (c) melted at 570–470°C, (d) melted at 750–570°C.

indicate that the issue of whether the melt experiences a LLSC has significant effects on the solidification behaviours.

Figure 4 shows the morphology of the phases, the size of primary phase (Bi_2Te) in the four samples decreases gradually, and the amount of eutectic phase in sample A is more than that in other samples. Moreover, the morphology of the primary phase was converted from dendrites into randomly arranged equiaxed grains after the melt experienced LLSC. Figure 5 shows the morphology of eutectic phase and it can be seen that the structures in sample B, C and D are finer than sample A.

4. Discussion

As the resistivity is one of the structurally sensitive parameters, the DC four-probe technique has been proved to be effective for exploring liquid alloy structures and their changing patterns, with the results in good agreement with those of DSC, internal friction and θ–θ X-ray diffraction [10,21–22]. It is reasonable to assume that the abnormal behaviours of resistivity versus temperature reflect two irreversible LLSCs happened in Bi–10wt%Te melt.

Some results of recent works [23–30] suggested that the structures of some liquid alloys and pure metals (such as Al–Si, Sn–Pb, Ga, Bi, etc.) may be micro-heterogeneous in the continuous heating procedure, and there exist a lot of microdomains (even unsolved particles) in the melt. Some investigators assumed that

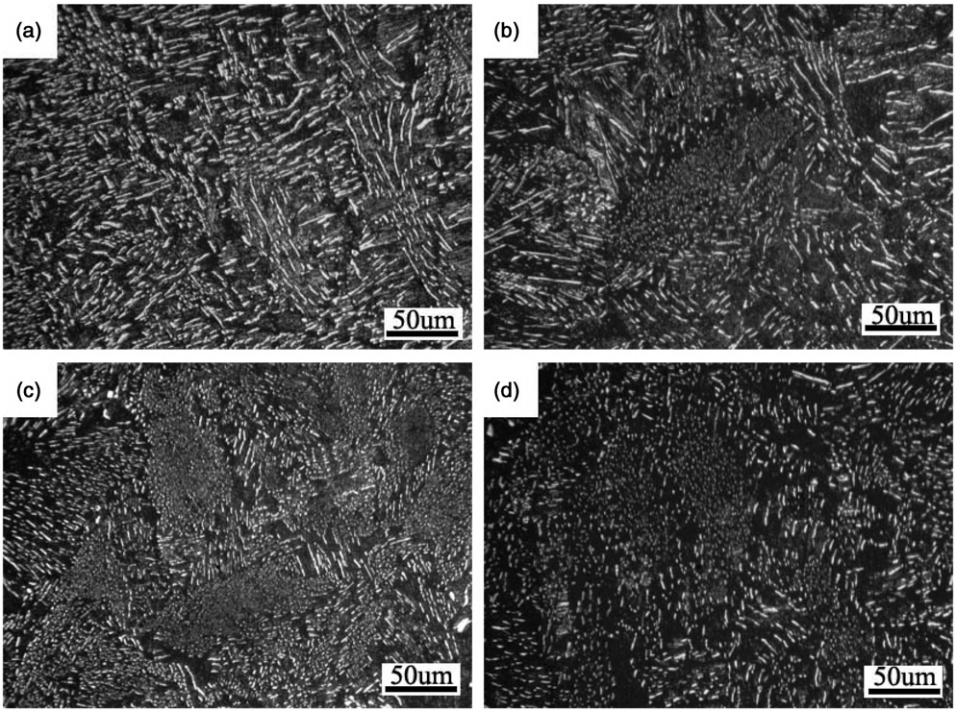

Figure 5. Magnification image of Bi–10wt%Te eutectic structures: (a) melted at 470°C, (b) melted at 570°C, (c) melted at 570–470°C, (d) melted at 750–570°C.

the micro-heterogeneous states are metastable or non-equilibrium thermodynamically [23,26]. Therefore, we can assume that liquid Bi–10wt%Te alloy consists of short-range orders (SROs) similar to eutectic and primary phase (Bi_2Te). When temperature is elevated continuously to the turning point, the kinetic energy of the atoms becomes high enough to overcome the energy barrier. The temperature range 497–550°C similar to that deduced by the broken up of the bonds of Bi–Bi, the resistivity in our experiments is ascending non-linear, while it is descending non-linear caused by the break up of the bonds of Bi–Bi. So, we consider that in Bi–10wt%Te the SROs similar to eutectic start to break up from 497°C, and end at 550°C. Then with the temperature increasing to 639°C, the SROs similar to primary phase (Bi_2Te) begin to break up and end at 708°C. Thus, the previous bonds are broken and new bonds are generated so that the structure transition of local SROs take place, or part/all of the previous bonds are broken so that local SROs dissolve to make the high-temperature liquid more disordered.

During solidification, the melt that fails to undergo a LLSC has a large number of relatively big clusters. Through fluctuations in structure and energy, those clusters can easily extend to the critical size of crystal nucleus under a low level of undercooling. Moreover, parts of those retained clusters in the melt have a similar structure to the solid phases, and this structural relation between the solid phases and the clusters enables the clusters to be easily deposited on the sites of the corresponding solid crystal lattice, hence, the nucleus can grow up under minor

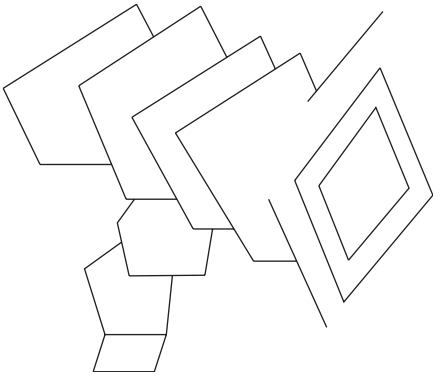

Figure 6. Sketch of dendrite of non-metal or metalloid.

energy fluctuation. This made it convenient for primary phase to nucleate, so the primary phase can easily grow to larger size. However, after experiencing a LLSC, the melt is hard to nucleate because the smaller and more homogeneous clusters are distinct from the solid phase. As a result, the melt needs a greater level of undercooling to nucleate. Based on the classical nucleation theory, the rate of nucleation is sensitive to undercooling, and the rate of nucleation proliferates with an exponential function of ΔT^2, so a higher nucleation rate I is obtained.

As mentioned above, there are two types of SROs in the melt not much above liquidus, one similar to eutectic and the other similar to primary phase. For melt A, having both of the SROs, when the temperature cooled below liquidus, primary phase can easily grow; when the temperature descends below eutectic line, eutectic will precipitate rapidly. For melt B, C and D, the dissolution of SROs similar to eutectic makes the nucleation of eutectic more difficult, which is propitious to grow for primary phase. So, the eutectic grains are finer, and the amount of primary phase is much more than that in sample A. For melt D, the dissolution of SROs makes the nucleation of primary phase more difficult, which causes the finest primary phase.

As shown in Figure 6, the dendrite of non-metal or metalloid is like polygon structures deposit in lamellar. On solidification, the primary phase in the four samples grew as the dendrite style at first. Nevertheless, for the smaller effective partition coefficient in the melt experienced LLSC [31], the primary phase in melt B and C would reject out more Te atom than in melt A, besides in melt D it would reject even more, and aggravated the local solute enrichment at the root of the dendritic arm; thus, the melting point here would be decreased. Therefore, by a relatively lower thermal fluctuation, the secondary arm would be melted just at the root of it and separated from the main stalk. So, as seen from Figure 4, the primary phase in sample A is totally dendritic, in sample B and C is most dendritic, while in sample D, only one half is dendritic, the other half is equiaxed.

5. Conclusions

(1) The anomalous changes on the ρ–T curves suggest that two irreversible LLSCs occur within the temperature ranges of 497–550°C and 639–708°C.

The structure changes can be attributed to the dissolution of the eutectic and Bi_2Te type of SROs, respectively.

(2) The LLSC resulted in the increase of undercooling, the refinement of grains and further led to the local solute enrichment and the secondary arm break up from the trunk; finally, it caused the morphology of solidified Bi_2Te change from dendrite to equiaxed.

Acknowledgements

This work has been supported by National Natural Science Foundation of China (Grants No. 50371024 and 50571033) and by the Provincial Natural Science Foundation of Anhui (Grants No. 070416234 and 070414178).

References

[1] M. Johnsson and L. Backerud, Z. Metallkd. **83**, 774 (1992).
[2] O. Tatsuya and K. Masayuki, J. Jpn Inst. Metals **56**, 1064 (1992).
[3] O. Tatsuya and K. Masayuki, J. Jpn Inst. Metals **58**, 1311 (1994).
[4] X. Bian and J. Ma, Chin. J. Mech. Eng. **5**, 176 (1992).
[5] F.S. Yin, X.F. Sun, J.G. Li, H.R. Guan, and Z.Q. Hu, Scripta Mater. **48**, 425 (2003).
[6] V.I. Danilov and I.V. Radchenko, Zh. Exp. Teor. Fiz. **7**, 1158 (1937).
[7] P.S. Popel, M. Calvo-Dahlborg, and U. Dahlborg, J. Non-Crystal. Solids **353**, 3243 (2007).
[8] F.Q. Zu, Z.G. Zhu, L.J. Guo, B. Zhang, J.P. Shui, and C.S. Liu, J. Phys. Rev. B **64**, 180203 (2001).
[9] U. Dahlborg, M. Calvo-Dahlborg, P.S. Popel, and V.E. Sidorov, Eur. Phys. J. B **14**, 639 (2000).
[10] Z.G. Zhu, F.Q. Zu, L.J. Guo, and B. Zhang, Mater. Sci. Eng. A **370**, 427 (2004).
[11] X.F. Li, F.Q. Zu, H.F. Ding, J. Yun, L.J. Liu, Q. Li, and Y. Xi, Physical B **358**, 126 (2005).
[12] Y.Q. Wu, X.F. Bian, Q.G. Meng, Y. Zhao, T. Mao, and Y.N. Zhang, Mater. Lett. **61**, 078275 (2006).
[13] F.Q. Zu, Z.G. Zhu, B. Zhang, Y. Feng, and J.P. Shui, J. Phys- Condens. Mat. **13**, 11435 (2001).
[14] F.Q. Zu, R.R. Shen, Y. Xi, X.F. Li, G.H. Ding, and H.M. Liu, J. Phys- Condens. Mat. **18**, 2817 (2006).
[15] F.Q. Zu, Z.G. Zhu, L.J. Guo, X.B. Qin, H. Yang, and W.J. Shan, J. Phys. Rev. L. **89**, 125505 (2002).
[16] Y. Xi, F.Q. Zu, and L.J. Liu, Kovove Mater. **43**, 432 (2005).
[17] F.Q. Zu, G.H. D, and X.F. Li, J. Cryst. Growth **310**, 397 (2008).
[18] X. Bian and W. Wang, Mater. Lett. **44**, 54 (2000).
[19] D.M. Rowe and C.M. Bhandarim, *Modern Thermoelectrics* (Reston Publishing, Reston, 1983).
[20] D.M. Rowe, *CRC Handbook of Thermoelectrics* (CRC Press, New York, 1995).
[21] L. Wang, X. F. Bian, and J.T. Liu, Phys. Lett. A **326**, 429 (2004).
[22] Y. Zhao, X.F. Bian, X.B. Qin, J.Y. Qin, and X.X. Hou, Phys. Lett. A **356**, 386 (2006).
[23] P.S. Popel, M. Calvo-Dahlborg, and U. Dahlborg, J. Non-Crystal. Solids. **353**, 3243 (2007).
[24] U. Dahlborg, M. Calvo-Dahlborg, P.S. Popel, and V.E. Sidorov, Eur. Phys. J. B **14**, 639 (2000).

[25] E.G. Jia, A.Q. Wu, L.J. Guo, C.S. Liu, W.J. Shan, and Z.G. Zhu, Phys. Lett. A **364**, 505 (2007).
[26] P.S. Popel, O.A. Chikova, and V.M. Matveev, High Temp. Mater. P-US **14**, 219 (1995).
[27] U. Dahlborg, M. Besser, M. Calvo-Dahlborg, G. Cuello, C.D. Dewhurst, M.J. Kramer, J.R. Morris, and D.J. Sordelet, J. Non-Crystal. Solids **353**, 3005 (2007).
[28] Maria Dutkiewicz and Edward Dutkiewicz, Electrochim. Acta **51**, 2346 (2006).
[29] S. Mudry and I. Shtablavyi, J. Non-Crystal. Solids **352**, 4287 (2006).
[30] S.V. Prokhorenko, High Temp. **43**, 700 (2005).
[31] F.Q. Zu, J. Chen, X.F. Li, L.N. Mao, Y.C. Liu, J. Mater. Res. (In press).